



Apolipoprotein E4 facilitates transfection of human monocyte-derived dendritic cells by lipid nanoparticles

Izabella Lambart^{a,b}, Hannah Zaryouh^c, Jonas Van Audenaerde^c, Dana Liu^c,
Delphine Quatannens^c, Eva Lion^d, Stefan Schiller^a, Simon Geissler^a, Evelien Smits^c,
Karsten Mäder^{b,*}

^a Merck Healthcare KGaA, Global Drug Product Development, Darmstadt, Germany

^b Martin Luther University Halle-Wittenberg, Institute of Pharmacy, Faculty I of Natural Sciences, Halle/Saale, Germany

^c Center for Oncological Research (CORE), Integrated Personalized and Precision Oncology Network (IPPON), Faculty of Medicine and Health Sciences, University of Antwerp, Wilrijk, Belgium

^d Laboratory of Experimental Hematology (LEH), Vaccine & Infectious Disease Institute (VAXINFECTIO), Faculty of Medicine and Health Sciences, University of Antwerp, Wilrijk, Belgium

ARTICLE INFO

Keywords:

Lipid nanoparticles
eGFP mRNA
MS2 RNA
Dendritic cell
Transfection
Apolipoprotein
Electroporation

ABSTRACT

The use of mRNA as a therapeutic drug class is a safe and fast alternative to viral vector or plasmid DNA therapies. Nevertheless, free mRNA will be rapidly degraded after administration to the body and only reach the cytosol of desired cells with difficulty. Lipid nanoparticles (LNP) safely deliver mRNA to cells of interest and can be used in the treatment of different diseases. Dendritic cells are the primary antigen-presenting cells and important for mRNA vaccine delivery. Efforts to increase LNP transfection of these cells are necessary and can be achieved by different approaches. Here, we present apolipoprotein E4 addition to LNP administration as one mean of increasing LNP-mediated eGFP mRNA delivery to human monocyte-derived dendritic cells. We also show some steps in the preparation method for LNP optimization using MS2 RNA as a novel model nucleic acid.

1. Introduction

An advantage of using mRNA as a new technology for vaccination is that it avoids the risk of host genome integration by acting as an intermediate for protein translation, which occurs at the ribosomes present in the cell cytoplasm (Pardi et al., 2018; Verbeke et al., 2019). However, the use of free mRNA as therapy to engineer cells faces challenges like ribonuclease enzyme-mediated degradation and poor cellular uptake caused by cellular membrane electrostatic repulsion (Aldosari et al., 2021; Eygeris et al., 2022). An established method for mRNA delivery to cells is electroporation (EP), in which cell membrane integrity is temporarily disrupted by an electric field applied via voltage pulses. It results in high transfection efficiency combined with maintaining high cell viability for several cell types. It is suitable for clinical application to transiently engineer cells ex vivo, including dendritic cells as professional antigen-presenting cells of the immune system (Campillo-Davo et al., 2021). Complementary to the EP method, injecting free mRNA is

highly interesting to target cells in vivo. Regardless of its many advantages, EP can still elicit safety concerns because of the severe collateral damage associated with the high voltage required. Also, when considering the translation to the clinic for treatment of internal organs, it poses the problem of requiring surgical procedures (Sokolowska and Błachnio-Zabielska, 2019).

These issues can be overcome by formulating mRNA inside lipid nanoparticles (LNP), which will protect the nucleic acid and improve interaction with the mammalian cell membrane. The amphipathic nature of phospholipids in LNP facilitates membrane fusion and internalization by the cell, and provides a safer delivery to target cells (Kon et al., 2022; Sharma et al., 2024). Besides the cargo of interest, LNP usually comprise four lipid components: an ionizable cationic lipid (IL), a phospholipid, cholesterol, and a polyethylene glycol lipid (PEG-lipid) (Hald Albertsen et al., 2022). The IL plays an important role in payload encapsulation during production and its release inside target cells. Its protonation in acidic pH enables interaction with negatively charged

* Corresponding author.

E-mail addresses: izabella.lambart@merckgroup.com (I. Lambart), hannah.zaryouh@uantwerpen.be (H. Zaryouh), jonas.vanaudenaerde@uantwerpen.be (J.V. Audenaerde), dana.liu@uantwerpen.be (D. Liu), delphine.quatannens@uantwerpen.be (D. Quatannens), stefan.schiller@merckgroup.com (S. Schiller), simon.geissler@merckgroup.com (S. Geissler), evelien.smits@uantwerpen.be (E. Smits), karsten.maeder@pharmazie.uni-halle.de (K. Mäder).

<https://doi.org/10.1016/j.ijpharm.2025.125720>

Received 6 March 2025; Received in revised form 21 April 2025; Accepted 10 May 2025

Available online 11 May 2025

0378-5173/© 2025 The Author(s). Published by Elsevier B.V. This is an open access article under the CC BY license (<http://creativecommons.org/licenses/by/4.0/>).

nucleic acids during LNP particle formation. It also facilitates cargo release to the cytosol by electrostatic interaction with the anionic membrane of cellular endosomes. Furthermore, the neutral charge of an IL at physiological pH accounts for improved circulation time by preventing rapid clearance by immune cells (Gote et al., 2023; Hou et al., 2021; Schober et al., 2024). Phospholipids help to prevent nucleic acid cargo leakage by stabilizing the membrane and improve the cellular delivery of LNP. Cholesterol fills the gaps between phospholipids and maintains membrane integrity and rigidity (Cheng and Lee, 2016; Hald Albertsen et al., 2022; Schober et al., 2024). The addition of PEG-lipids to LNP formulations is related to the control of LNP aggregation and fusion, important for shelf-life stability; extended *in vivo* circulation time; and decreased vaccine immunogenicity. Usual PEG-lipid molar concentrations are below 2.5 %, since high concentrations can decrease RNA delivery to the cell (Kon et al., 2022; Wang et al., 2023).

A variety of manufacturing methods can be used to produce lipid-based nanoparticles, such as continuous self-assembly by precipitation, lipid film hydration and microfluidic mixing by different mixing technologies (e.g. staggered herringbone mixer or toroidal mixer) (Webb et al., 2022). A commonly chosen technique is microfluidics, which leads to high reproducibility and ensures consistency between batches by enabling precise control of process parameters (Lamparelli et al., 2025; Pareja Tello et al., 2025). Also, high flow rate microfluidic mixing is capable of achieving low polydisperse particles with high encapsulation efficiency because it allows RNA-containing aqueous phase and lipid-containing ethanolic phase blending to occur in a fast and consistent way (Schober et al., 2024). Microfluidic processes can be run on chip-based or capillary-based platforms, with several production chips with different morphologies and designs available for chip-based devices (Mehta et al., 2023). LNP preparation methods are important and should be optimized for the desired payload because they directly impact LNP characteristics related to biodistribution and therapeutic effects, such as hydrodynamic diameter, polydispersity index and nucleic acid encapsulation efficiency (Maeki et al., 2022).

Dendritic cells (DC) play a pivotal role in activating the immune system to fight infections and cancer by presenting associated antigens to T cells. Therefore, they are an ideal target for mRNA LNP vaccines and have been the aim of different nanoparticles for nucleic acid delivery (Das et al., 2024; Das et al., 2023; Hobo et al., 2013; Shi et al., 2017). Apolipoprotein E is a plasma lipoprotein with three major isoforms, namely apolipoproteins E2, E3 and E4. It is produced in most organs and found in significant quantities in the liver, brain, and muscle, among other organs. Also, it is present in high concentrations in the interstitial fluid as a secretion product of different cell types, such as macrophages and smooth muscle cells (Huang and Mahley, 2014; Mahley, 1988). Apolipoprotein E can bind LNP and facilitate their cellular internalization via low-density lipoprotein receptors (LDLR). Therefore, we believe that its addition during *in vitro* LNP-mediated delivery to DC can better simulate physiological conditions and should be further investigated, especially with regard to human DC since previous reports showed no influence of apolipoprotein in LNP-mediated delivery to murine DC (Zhang et al., 2024). Furthermore, it has been demonstrated that apolipoprotein E4 (ApoE), was essential for mRNA delivery to T cells by a proprietary LNP composition. Interestingly, CAR-mRNA LNP delivery outperformed electroporation with regards to prolonged efficacy *in vitro* (Kitte et al., 2023).

In this study, we investigated the impact of ApoE on LNP-mediated transfection of human monocyte-derived DC. LNP and electroporation-mediated delivery were compared to investigate the possibility of transferring the reported superior performance of LNP for T cell delivery in presence of ApoE to DC delivery. The lipid composition of patisiran (trade name Onpattro®) was used as a starting point for mRNA delivery to DC. The choice was based upon the fact that patisiran was designed to be internalized by interaction with the same receptor that has high affinity for ApoE (Akinc et al., 2019; Johnson et al., 2014). Also, it was the first FDA-approved siRNA-LNP drug, developed for the treatment of

hereditary disease transthyretin-mediated amyloidosis (Akinc et al., 2019), and has been on the market for several years. MS2 RNA was used as a model RNA for investigation of different production parameters before switching to eGFP mRNA to monitor transfection efficiency.

2. Materials and methods

2.1. Materials

(6Z,9Z,28Z,31Z)-Heptatriaconta-6,9,28,31-tetraen-19-yl 4-(dime-thylamino) butanoate (D-Lin-MC3-DMA) was bought from AmBeeD, Arlington, USA. 1,2-distearoyl-*sn*-glycero-3-phosphocholine (DSPC) was bought from Avanti Polar Lipids Inc., Alabaster, USA. 3 β -Hydroxy-5-cholesten/5-Cholesten-3 β -ol (cholesterol, Sigma Grade \geq 99 %), modified Dulbecco's Phosphate buffered saline 10x, without MgCl₂ and CaCl₂ (used for LNP dialysis), Triton™ X-100, 1,2-Dimyristoyl-*rac*-glycero-3-methoxypolyethylene glycol-2000 (DMG-mPEG-2000), sucrose, citric acid monohydrate, and ethanol were bought from Merck KGaA, Darmstadt, Germany. Sodium chloride solution (0.9 %) was bought from PanReac AppliChem ITW Reagents. CleanCap® FLuc mRNA (5moU) (luciferase mRNA) and CleanCap® EGFP mRNA (5moU) (eGFP mRNA) were bought from TriLink Biotechnologies, San Diego, USA. MS2 RNA from bacteriophage MS2 (MS2 RNA) was bought from Roche Diagnostics GmbH, Mannheim, Germany. Human apolipoprotein E4 Recombinant protein, PeproTech® and LIVE/DEAD™ Fixable Near-IR were bought from Thermo Fisher Scientific. Phosphate buffered saline (PBS) buffer (used for cell culture), L-glutamine, sodium pyruvate, penicillin/streptomycin and cell medium RPMI 1640 were bought from Gibco. Human serum albumin was bought from Sigma Aldrich. PGE₂ and TNF α were bought from BioTechne, Wiesbaden-Nordenstadt, Germany.

Human immature DC are manufactured as described elsewhere (Lion et al., 2011). Peripheral blood mononuclear cell required for production of these DC are provided by the Red Cross Flanders, approved by the Ethics Committee of the University of Antwerp (Antwerp, Belgium) and the Antwerp University Hospital (Antwerp, Belgium) under the reference number 5488.

2.2. LNP formulation and production

LNP were produced by mixing D-Lin-MC3-DMA, DSPC, cholesterol and DMG-mPEG-2000 (50:10:38.5:1.5) in ethanol with luciferase mRNA, eGFP mRNA, or MS2 RNA in citrate buffer (50 mM, pH 3). The mixing process occurred in a microfluidic system (Sunshine model, previously known as Automated Nanoparticle System, Unchained Labs, Royston, United Kingdom), with a total flow rate (TFR) of 7 mL/min, a flow rate ratio (aqueous:ethanolic) of 3:1, a total lipid concentration of 20 mM, N/P ratio of 6. Production occurred either in the junction chip (100 μ m or 190 μ m etch depth, Unchained Labs, Royston, United Kingdom) or the trident chip (Unchained Labs, Royston, United Kingdom). For a TFR of 7 mL/min, calculated Reynolds numbers were 1420, 762 and 303 for the 100 μ m, 190 μ m and trident chip, respectively. After production, LNP were dialyzed against PBS buffer, with or without addition of sucrose, using the dialysis system Spectra/Por® Float-A-Lyzer® G2 (Repligen, Massachusetts, USA) for 24 hours at 4 °C and 300 rpm. Buffer was exchanged after 2 and 6 hours.

2.3. LNP characterization

Hydrodynamic diameter and polydispersity index (PDI) were measured by dynamic light scattering (Zetasizer Nano ZS, Malvern Analytical GmbH, Kassel, Germany). Samples were diluted 50-fold in PBS buffer and measured in backscatter mode (173°), 3 \times 10 \times 10 s at 25.0 °C using cumulants fit (z-average and PDI). ζ -potential of selected samples was measured by laser Doppler anemometry (same instrument). Samples were diluted 50-fold in 10 mM NaCl solution (resulting pH of

7.2) and measured three times at 25.0 °C in a folded capillary cell (DTS1070) with automatic measurement duration and voltage selection, using the Smoluchowski model and General Purpose mode. pH was measured in a 780 pH Meter equipment attached to a LL Biotrode 3 mm WOC (Metrohm). Endotoxin concentration in selected samples was measured as EU per µg mRNA using the Endosafe Nexgen-PTS (Charles Rivers Laboratories). Samples were diluted 100-fold in endotoxin free water (Charles Rivers Laboratories) and analyzed in cartridges with 0.5–0.005 EU/mL sensitivity (PTS55005F, Charles Rivers Laboratories). Encapsulation efficiency (EE) and total nucleic acid recovery (TnaR) were obtained by fluorescence analysis with the Quant-iT™ Ribogreen™ RNA Assay Kit (Invitrogen, Thermo Fisher Scientific). Briefly, LNP were incubated in 96-well plates (FluoroNunc™ F96 MicroWell™ plate, Thermo Fisher Scientific) at 37 °C for 10 min in TE buffer, either pure or containing 1 % Triton™ X-100, to determine the fluorescence intensity of free mRNA (fmRNA) and total mRNA (tmRNA), respectively.

$$EE(\%) = \frac{tmRNA - fmRNA}{tmRNA} \times 100 \quad (1)$$

$$TnaR(\%) = \frac{tmRNA}{theoretical\ RNA\ concentration} \times 100 \quad (2)$$

2.4. *In vitro* assays

Human monocyte-derived DC were derived from CD14+ monocytes, isolated from buffy coats obtained via the Red Cross Flanders and approved by the UAntwerp – Antwerp University Hospital Ethical Committee under reference number 5488 (Smits et al., 2016). ApoE was dissolved in PBS buffer to a concentration of 50 µg/mL and stored at –20 °C until further use. Immature human monocyte-derived DC were seeded into a 6-well plate (1 x 10⁶ cells/well) and incubated at 37 °C with eGFP mRNA LNP in RPMI 1640 medium in the presence of the maturation cytokines PGE₂ (1 µg/mL) and TNFα (20 ng/mL) and without serum for 2 hours. Following 2-hour incubation, an equal volume of RPMI 1640 containing 5 % human serum albumin, 2 % penicillin/streptomycin, 2 % L-glutamine, 2 % sodium-pyruvate, 1 µg/mL PGE₂, and 20 ng/mL TNFα were added to the plate to bring the final serum concentration to 2.5 %. LNP were thawed at room temperature before addition to the wells for a total of 2 or 8 µg eGFP mRNA encapsulated in LNP. In experiments where ApoE was used, it was added to achieve 1 µg/well immediately before transfection with LNP. EP using free 2 µg eGFP mRNA was performed on a Gene Pulser Xcell device (Biorad) for 2 x 10⁶ cells/well, as previously described (Smits et al., 2016). Fluorescence signal was measured by flow cytometry (FACS Lyric) 48 hours post-transfection and analyzed with FlowJo™ v10.10.0. The gating strategy is described in Fig. S1.

2.5. Investigation of LNP frozen storage stability

LNP were dialyzed against PBS buffer containing sucrose in concentrations ranging from 0.025 to 0.1 g/g before storage. The particle size distribution and EE were determined as described in 2.3 after dialysis and after storage at –80 °C for one week or four weeks.

2.6. Statistical analysis

All experiments were performed with at least 3 independent donors, unless otherwise stated. Differences in %eGFP positive cells and ΔMFI between experimental conditions were statistically analyzed using a non-parametric Mann-Whitney *U* test. GraphPad Prism 10 was used for data comparison and artwork. All statistical analyses were performed in JMP Pro 17. P-values below 0.05 were considered statistically significant.

3. Results

3.1. MS2 RNA LNP consistently had size below 90 nm, PDI below 0.2 and EE above 90 %

To investigate process robustness and establish the acceptance criteria of future experiments, mean hydrodynamic diameters and EEs were compared for 16 different MS2 RNA LNP batches produced with the 190 µm chip using the same parameters. PDI acceptance criteria was not determined, since PDI below 0.2 is already well accepted as indicative of good sample quality. As presented in Fig. 1, mean values of hydrodynamic diameter, PDI, EE and TnaR were 74 nm, 0.15, 97 % and 73 %, respectively. Hydrodynamic diameter range maximum and minimum values were 86 and 59 nm, respectively, and served as particle size acceptance criteria for LNP manufacturing optimization. Since lowest measured EE was 94 %, 84 % was defined as the lowest accepted EE, taking into consideration that previous investigation of the Ribogreen assay reproducibility showed ± 10 % variation for MS2 RNA (data not shown).

3.2. Most efficient LNP production achieved with 190 µm junction chip

To assess the impact of production chip on production efficiency, three chips with different geometries were selected to produce MS2 RNA LNP. As shown in Fig. 2, production with the 100 µm and 190 µm junction chips led to mean hydrodynamic diameters inside the desired range for MS2 RNA LNP, whereas production with the trident chip resulted in particles above 86 nm. PDI was also higher after producing with the trident chip, but a sufficient sample homogeneity was still achieved (PDI < 0.2). EE was higher than 95 % for LNP produced with both junction chips, while production with the trident chip led to an EE of around 70 %.

3.3. At least 0.075 g/g sucrose in PBS buffer was needed to keep particle size within determined range after LNP frozen storage

Freezing the LNP dispersion enables shipment without the worry about possible mRNA or lipid degradation by hydrolysis but requires a cryoprotectant to maintain the initial properties of the particles with minimal variation. To determine the lowest cryoprotectant concentration in buffer which provides sufficient stabilization, MS2 RNA LNP were produced and dialyzed against PBS buffer, either pure or with addition of sucrose in a concentration ranging from 0.025 to 0.10 g/g. While the lowest concentration of sucrose (0.025 g/g) was already sufficient to maintain PDI and EE close to the values after dialysis, at least 0.075 g/g sucrose was necessary to keep particle size within the assessed hydrodynamic diameter range of MS2 RNA LNPs (Fig. 3). Interestingly, particle size increase after freezing was observed for all storage buffers.

3.4. Defined production parameters led to similar results for different payloads

Ultimately, the optimization performed with MS2 RNA to establish a highly efficient LNP production setup would need to be transferred to LNP encapsulating mRNA encoding for a marker protein that enables a readout for *in vitro* testing. Therefore, the 190 µm junction chip was used to investigate the suitability of MS2 RNA LNP production parameters to manufacture LNP containing eGFP or luciferase mRNA (Fig. 4).

3.5. ApoE improved human DC transfection via LNP

It has been shown that LNP outperformed electroporation in a specific setup for effective T cell transfection, which required the presence of ApoE (Kitte et al., 2023). Here, we investigated ApoE impact on LNP transfection of human DC and compared mRNA delivery via LNP versus via EP. Since previous results showed no impact of DC maturation status

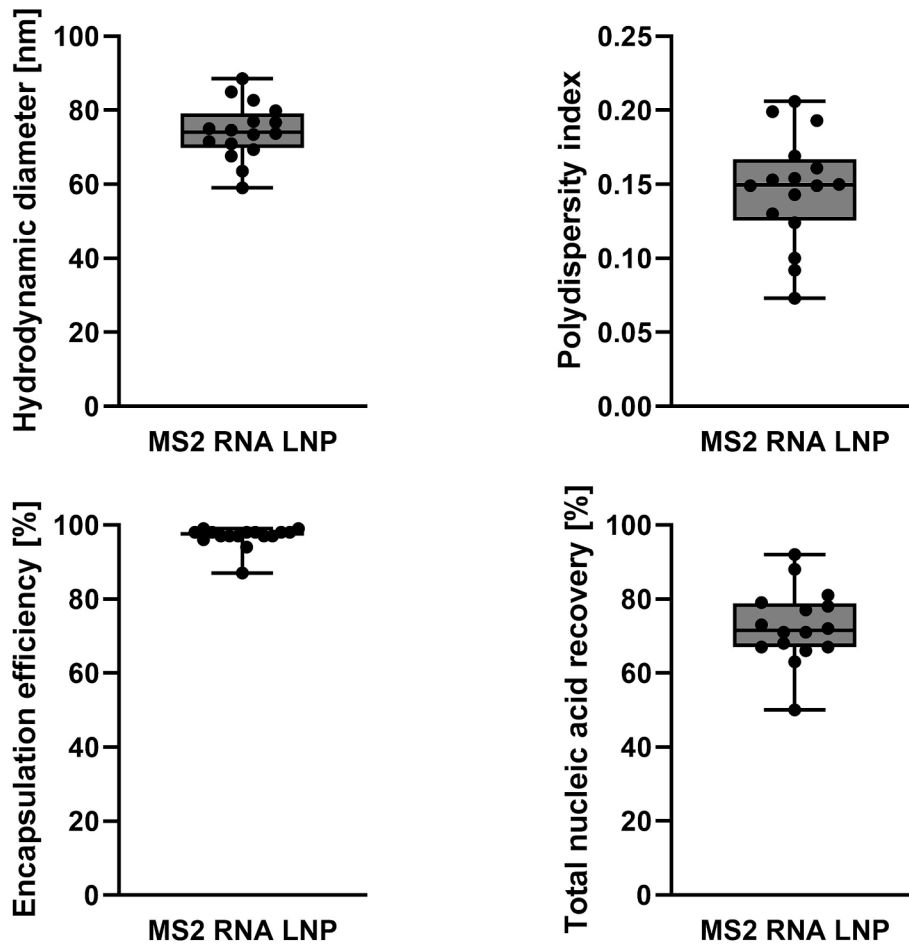


Fig. 1. Mean hydrodynamic diameters (top left), PDI values (top right), EE (bottom left) and TnaR (bottom right) for MS2 RNA LNP. The average of mean LNP hydrodynamic diameter was 74 nm. The average of mean PDI values were below 0.2. EE and TnaR were consistently above 90 % and 60 %, respectively. Data are expressed as mean \pm range (n = 16).

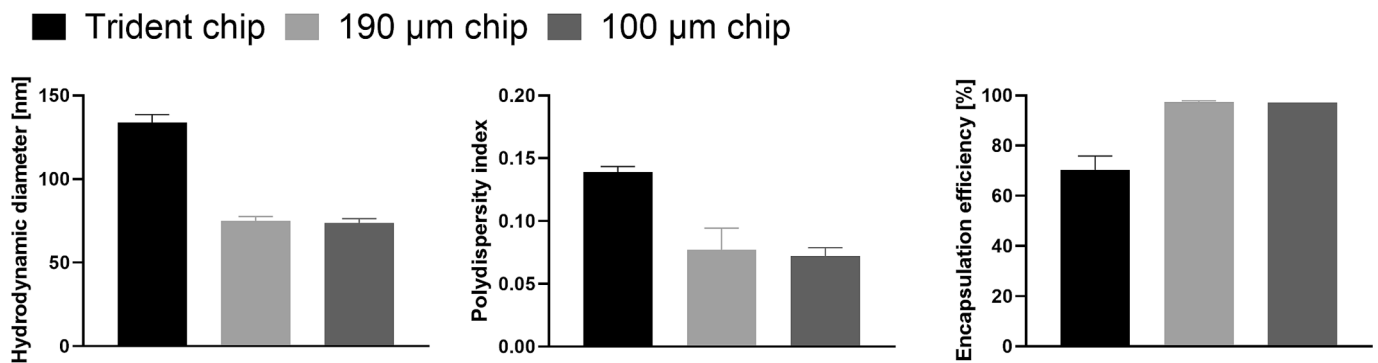


Fig. 2. Impact of different production chips on hydrodynamic diameter (left), PDI (center) and EE (right) of MS2 RNA LNP. Hydrodynamic diameter of LNP produced using the trident chip was almost twice as high as those obtained for particles produced with junction chips. Monodisperse dispersions were obtained regardless of the used chip type, as demonstrated by the PDI values below 0.2. Higher EEs were obtained when junction chips were used. Data are expressed as mean \pm SD (n = 3).

on LNP delivery (Fig. S2, Supplementary Information), immature DC were selected and incubated with LNP containing eGFP mRNA (delivered frozen in PBS buffer containing 0.1 g/g sucrose at pH 7.3; hydrodynamic size = 77 nm, PDI = 0.16, ζ -potential = -4.95 mV, encapsulated mRNA = 85 μ g/mL, EE = 99 % and endotoxin concentration = < 0.005 EU/ μ g_{mRNA}) with or without the addition of ApoE for a total of 48 hours. Although ApoE addition led to an increase in Δ MFI and %eGFP positive cells compared to LNP-mediated delivery in the

absence of ApoE, the results obtained for EP delivery were still higher at 1 μ g eGFP mRNA. Results showed a high percentage of live cells at 48 hours post-transfection with or without the presence of ApoE, confirming that the majority of cells maintain membrane integrity (Fig. 5).

4. Discussion

LNP manufacturing conditions play an important role in tuning the

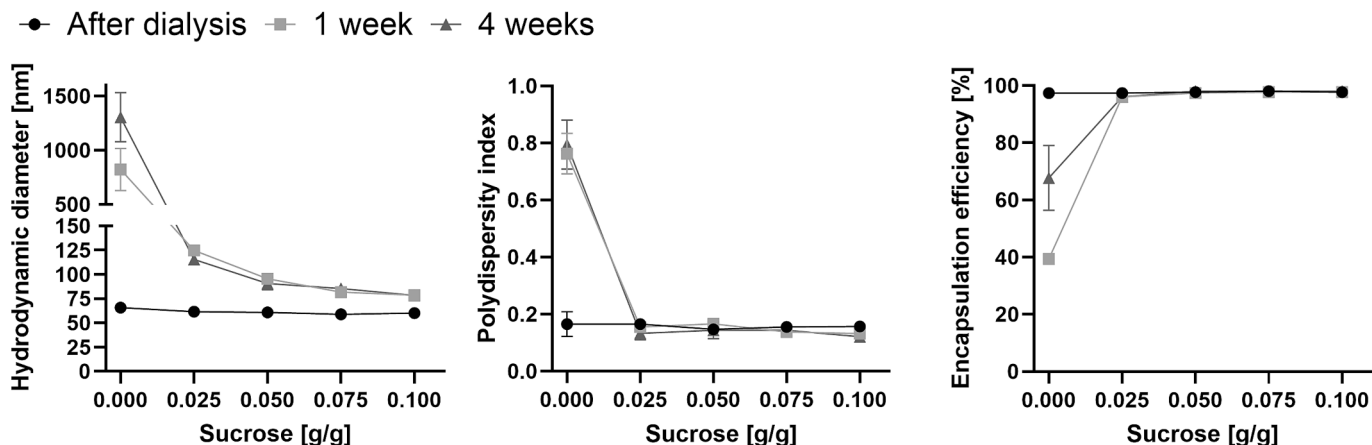


Fig. 3. Effect of sucrose concentration in storage buffer on LNP size (left), PDI (center) and EE (right). Addition of sucrose, regardless of concentration, was necessary to maintain PDI and EE in the same range as those of fresh samples. An increase in hydrodynamic diameter was observed for all samples after freezing but remained below 86 nm when buffer with at least 0.075 g/g sucrose was used. Data are expressed as mean \pm SD ($n = 3$).

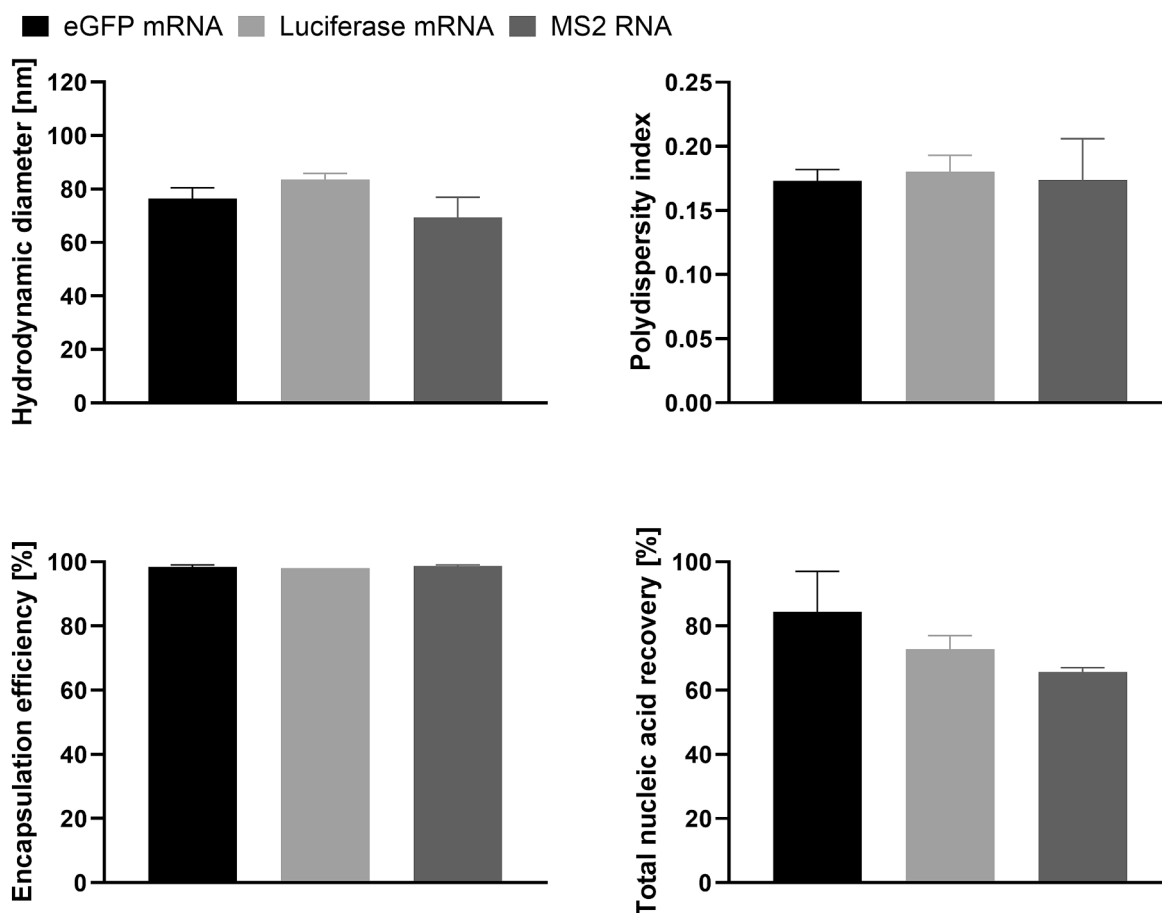


Fig. 4. Impact of different RNA loads on mean hydrodynamic diameters (top left), PDI values (top right), EE (bottom left) and TnaR (bottom right). Transferring the LNP production parameters optimized with MS2 RNA to eGFP or luciferase mRNA led to particles with similar hydrodynamic diameters, PDI values and EE. TnaR was different for each payload, with the lowest recovery for MS2 RNA at 65%. Data are expressed as mean \pm SD ($n = 3$).

particles to achieve desired characteristics. Here, the lipid composition of patisiran was used for the encapsulation of MS2 RNA in LNPs. To our knowledge, this is the first time that a publication has reported this RNA as LNP payload and presented it as a suitable model for production process development. MS2 RNA LNP mean particle size average was 74 nm with a narrow range of 59 to 86 nm (16 batches produced with a 190 μ m junction chip). This size range enables sterile filtration since the

largest intensity-weighted mean particle size (86 nm) was about 2.5-fold lower than the filter pore size (0.2 μ m). Mean PDI obtained after analysing 16 samples was 0.15 and EE was above 90%. While reports on nucleic acid recovery considering the initial RNA concentration are not commonly found in the literature, we agree that they are a fundamental tool to determine nucleic acid loss during the LNP production, as stated by (Schober et al., 2024). Our results of TnaR were consistently above

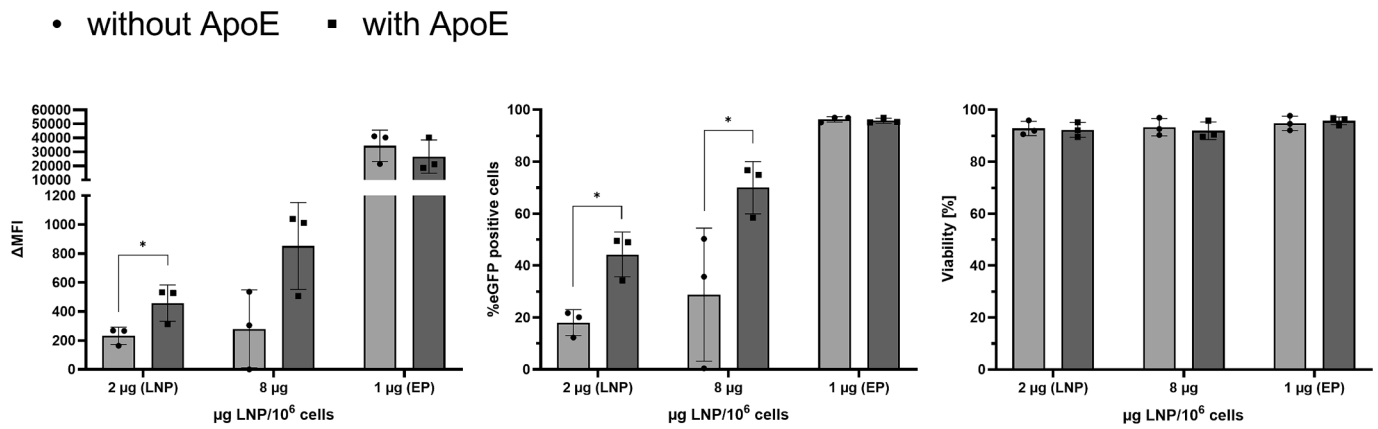


Fig. 5. LNP-mediated delivery was increased by apolipoprotein E4 addition but was inferior to EP. For LNP-mediated delivery, a dose-dependent effect on the amount of expressed eGFP within a cell (left) and number of eGFP-expressing cells (middle) was observed. Although a high percentage of eGFP positive cells was achieved with 8 μ g eGFP mRNA via LNP delivery, EP performed better at 1 μ g eGFP mRNA. For flow cytometry-based viability analysis (right), DC transfected with LNPs or via EP with/without the presence of ApoE were stained with a fixable live/dead viability dye and analyzed by flow cytometry 48 h post-transfection. The percentage of viable cells was determined based on exclusion of the viability dye. ApoE = apolipoprotein E4, EP = electroporation, LNP = lipid nanoparticle. Data are expressed as mean \pm SD for three independent donors. Statistically significant differences were calculated using a non-parametric Mann-Whitney *U* test. * = $p < 0.05$.

60 % for MS2 RNA, indicating good manufacturing conditions and low nucleic acid loss.

Comparable particle size distribution and EE was achieved when using a chip with a junction size of 100 μ m instead of 190 μ m. In contrast, using a trident chip led to particles with considerably larger mean hydrodynamic diameter (134 nm) and lower EE. The different channel geometries between both junction chips and the trident chip are likely the cause for the distinct results obtained. Adjustments in production parameters, such as increasing TFR, might be needed to achieve a similar mixing efficiency and to generate LNP below 86 nm in the trident chip, but this investigation was not in the scope of this work. Our experience showed the 190 μ m junction chip to be less prone to blockage due to its broader etch depth, which resulted in less cleaning efforts and faster production when compared to the 100 μ m junction chip (data not shown).

Storage and transport temperature needs to be considered when formulating LNP. The lipid components used to encapsulate MS2 RNA were based on the patisiran formulation, which was designed to deliver a small interfering RNA (siRNA) to hepatocytes for the treatment of transthyretin-mediated amyloidosis (Akinc et al., 2019). siRNA products can be stored as liquid formulations at 2 to 8 $^{\circ}$ C because higher chemical stability can be achieved by structural modifications (Oude Blenke et al., 2023), while two licensed mRNA vaccines for COVID-19, mRNA-1273 (Moderna) and BNT162b2 (BioNTech-Pfizer), still need below zero temperatures for storage and delivery (−15 to −25 $^{\circ}$ C and −60 to −90 $^{\circ}$ C, respectively) (Hou et al., 2021). It has been previously shown that addition of sugars to the formulation is suitable to avoid aggregation and efficacy reduction during LNP frozen storage (Ball et al., 2017). Therefore, we decided to study the ideal sugar concentration needed to stabilize MS2 RNA LNP at frozen temperatures. During initial investigations, abrupt increase in particle size after one week was avoided when 0.1 g/g sucrose was present in formulations stored at −80 $^{\circ}$ C, which could not be equally achieved for formulations stored at −20 $^{\circ}$ C or containing D(−)-mannitol instead of sucrose (data not shown). Hence, we studied the impact of different sucrose concentrations in storage buffer (PBS buffer) on MS2 RNA LNP stability at −80 $^{\circ}$ C. PDI and EE could be maintained in the same range as those of fresh samples regardless of sucrose concentration, but at least 0.075 g/g sucrose in PBS was needed to avoid LNP hydrodynamic diameter to increase above the highest end of the determined size range (86 nm). These findings align with previously reported sucrose concentrations of 10 % (w/v) for TT3 and D-Lin-MC3-DMA-based LNP in PBS and 8 % (w/v) for the mRNA-

1273 COVID-19 vaccine in tris buffer (Kim et al., 2023).

Transferring the production protocol optimized with MS2 RNA LNP to eGFP and luciferase mRNA was the last step needed before particles could move to *in vitro* testing. All tested LNP had similar hydrodynamic diameters, PDI and EE values despite their diverse chain lengths (eGFP mRNA: 997 bases, luciferase: 1922 bases and MS2 RNA: 3569 bases). Interestingly, our results showed TnAR values to decrease with the increase in chain length. This differs from the findings of (Schober et al., 2024), in which eGFP mRNA was encapsulated with lower recovery than the larger luciferase mRNA. Also, TnAR values for luciferase (72 %) and eGFP mRNA (84 %) were higher than the reported EE_{input} (encapsulation efficiencies based on input RNA concentration) values that were calculated in the mentioned study (around 50 % and 40 % for luciferase mRNA and eGFP mRNA, respectively). For a more concrete comparison, using their formula on our data, luciferase mRNA and eGFP mRNA would have 60 % and 78 % EE_{input} %, respectively (data not shown). However, our investigation occurred at an ionizable lipid to RNA ratio (N/P ratio) of 6, ten times lower than theirs, and we used a total lipid concentration twenty times as high as their tested concentration of 1 mM. This variation in lipid amount present during LNP manufacturing is a possible reason for the differences observed and aligns with their report that increasing the total lipid concentration to 10 mM while maintaining N/P ratio at 60 improved nucleic acid recovery.

It has been shown that LNP delivery can outperform EP for CAR-encoding mRNA delivery to human T cells when an undisclosed proprietary lipid composition optimized for T cells was used in the presence of ApoE4 (Kitte et al., 2023). Here, immature human DC were selected to investigate if addition of ApoE would increase transfection efficiency of LNP and even enable a range of transfection close to that of EP, especially considering that the lipid formulation of patisiran was originally designed for liver uptake by interaction with the LDLR, which has high affinity for ApoE (Johnson et al., 2014). eGFP mRNA LNP successfully transfected DC in a dose-dependent manner. Even in the absence of ApoE, 18 and 29 % eGFP positive cells were achieved for 2 and 8 μ g encapsulated mRNA delivered via LNP, respectively. In the presence of ApoE, DC viability was maintained while %eGFP positive cells and Δ MFI of LNP were increased in at least 2-fold, which is in alignment with studies showing ApoE enhancement of LNP uptake in HeLa cells (Akinc et al., 2010) but contradicts a finding reporting no ApoE influence on uptake in murine DC (Zhang et al., 2024). The difference in results for ApoE impact on DC transfection could be related to differences in experimental setup. The mentioned study investigated 0.1 μ g/mL ApoE

per 2.5×10^5 cells, the IL SM-102, N1-methylpseudouridine eGFP mRNA and murine DC for an incubation of 24 hours. Our study used $0.25 \mu\text{g}/\text{mL}$ ApoE per 2.5×10^5 cells, the IL D-Lin-MC3-DMA, 5-methoxyuridine eGFP mRNA and human DC for an incubation of 48 hours. In contrast, similarities in both studies might indicate which factors are less likely to be the cause of observed differences and will be briefly stated. The molar percentage of each lipid in composition was the same and more importantly, PEG lipid was set at 1.5 %, which is half the limit shown to decrease ApoE adsorption to LNPs (Kim et al., 2021). Also, the highest eGFP mRNA concentration delivered via LNP and used for comparison of ApoE influence was the same ($2 \mu\text{g}/2.5 \times 10^5$ cells).

Nevertheless, despite the increase in %eGFP positive cells and ΔMFI after ApoE addition LNP-mediated delivery to DC could not achieve the same observed for T cell delivery and did not outperform EP. In fact, compared to the lowest ΔMFI (approx. 2.6×10^4) obtained after EP delivery, ΔMFI achieved with the highest eGFP mRNA concentration tested was at least around 30-fold lower. The reason for LNP underperformance is unknown and could be related to an insufficient cellular uptake of particles, endosomal release or even unexpected distribution of eGFP mRNA outside the cytosol. Further investigation, as for example determining eGFP mRNA localization in cell after transfection by confocal imaging, are necessary to help identify the cause of difference between LNP and EP transfection but were not performed in this work. Despite not being comparable to EP, our results of 70 % eGFP positive cells obtained with $8 \mu\text{g}$ eGFP mRNA in LNPs in presence of ApoE were not only comparable to what has already been reported in literature for LNP-mediated delivery to DC (Zhang et al., 2024) but supports the importance of this lipoprotein for future investigations in human DC.

LNP optimization might be the key to increase particle uptake even more, if the aid of targeting moieties is unavailable, and might be closely related to formulation composition. For instance, the influence of the IL on DC uptake has been demonstrated when LNP produced with CL4H6 as the IL induced better transgene expression activity and maturation in DC than the patisiran IL D-Lin-MC3-DMA (Sasaki et al., 2022). Although some formulations for mRNA delivery to DC via LNPs have been reported in a recent review (Kim et al., 2024), we believe that there is still a need for further investigations on different means to improve DC transfection.

5. Conclusions

To the best of our knowledge, MS2 RNA was used for the first time in process development and optimization. It enabled the creation of a highly efficient LNP production setup to be transferred to fluorescent protein-encoding mRNA for *in vitro* experiments. For LNP production, optimal conditions were achieved when using the $190 \mu\text{m}$ junction chip and 0.075 to 0.1 g/g sucrose in PBS buffer for dialysis overnight. Production setup transfer from MS2 RNA to eGFP mRNA or luciferase mRNA led to similar hydrodynamic diameter, PDI and EE. Nucleic acid recovery after production is also presented and showed to decrease with the increase of payload chain length. Nevertheless, lowest obtained TnaR was above 60 %, indicating good manufacturing conditions with low nucleic acid loss. eGFP mRNA LNP were selected for *in vitro* assays, in which human DC transfection was shown to occur in absence of ApoE in a dose-dependent manner. The addition of ApoE led to increased ΔMFI and %eGFP positive cells, indicating that LNP transfection of DC is facilitated by this protein. The outperformance of LNP over electroporation in the presence of ApoE, observed for T cells (Kitte et al., 2023), could not be demonstrated for DC. Nevertheless, LNPs showed improved transfection efficiency in the presence of ApoE4, paving the way to further investigate these particles for *in vivo* and *ex vivo* applications.

CRedit authorship contribution statement

Izabella Lambart: Writing – original draft, Visualization, Project administration, Methodology, Investigation, Formal analysis,

Conceptualization. **Hannah Zaryouh:** Writing – review & editing, Visualization, Methodology, Formal analysis, Conceptualization. **Jonas Van Audenaerde:** Writing – review & editing, Visualization, Methodology, Investigation, Formal analysis, Conceptualization. **Dana Liu:** Investigation. **Delphine Quatannens:** Investigation. **Eva Lion:** Supervision, Resources. **Stefan Schiller:** Writing – review & editing, Supervision, Resources. **Simon Geissler:** Writing – review & editing, Supervision, Resources. **Evelien Smits:** Writing – review & editing, Supervision, Resources, Project administration. **Karsten Mäder:** Writing – review & editing, Supervision.

Declaration of competing interest

The authors declare the following financial interests/personal relationships which may be considered as potential competing interests: Izabella Lambart, Hannah Zaryouh, Jonas Van Audenaerde, Dana Liu, Delphine Quatannens, Stefan Schiller, Simon Geissler and Evelien Smits report financial support provided by European Commission within the Horizon Europe Framework Programme (HORIZON). Karsten Mäder reports a relationship with Merck Healthcare KGaA, Darmstadt, Germany that includes: consulting or advisory. Izabella Lambart, Stefan Schiller and Simon Geissler report a relationship with Merck Healthcare KGaA, Darmstadt, Germany that includes: employment. If there are other authors, they declare that they have no known competing financial interests or personal relationships that could have appeared to influence the work reported in this paper.

Acknowledgements

The presented work is part of the CANCERNA Consortium, publicly funded by the European Commission within the Horizon Europe Framework Programme (HORIZON) under the project ID 101057250. We thank Stefanie Peeters for technical assistance and Oliver Laukhart, Dogan Temel, Cornelia Roth and Olaf Tesch for shipment support.

Appendix A. Supplementary data

Supplementary data to this article can be found online at <https://doi.org/10.1016/j.ijpharm.2025.125720>.

Data availability

Data will be made available on request.

References

- Akinc, A., Maier, M.A., Manoharan, M., Fitzgerald, K., Jayaraman, M., Barros, S., Ansell, S., Du, X., Hope, M.J., Madden, T.D., Mui, B.L., Semple, S.C., Tam, Y.K., Ciufolini, M., Witzigmann, D., Kulkarni, J.A., van der Meel, R., Cullis, P.R., 2019. The Onpatro story and the clinical translation of nanomedicines containing nucleic acid-based drugs. *Nat. Nanotechnol.* 14, 1084–1087. <https://doi.org/10.1038/s41565-019-0591-y>.
- Akinc, A., Querbes, W., De, S., Qin, J., Frank-Kamenetsky, M., Jayaprakash, K.N., Jayaraman, M., Rajeev, K.G., Cantley, W.L., Dorkin, J.R., Butler, J.S., Qin, L., Racie, T., Sprague, A., Fava, E., Zeigerer, A., Hope, M.J., Zerial, M., Sah, D.W.Y., Fitzgerald, K., Tracy, M.A., Manoharan, M., Kotliansky, V., de Fougerolles, A., Maier, M.A., 2010. Targeted delivery of RNAi therapeutics with endogenous and exogenous ligand-based mechanisms. *Mol. Ther. : J. Am. Soc. Gene Ther.* 18, 1357–1364. <https://doi.org/10.1038/mt.2010.85>.
- Aldosari, B.N., Alfaghi, I.M., Almurshedi, A.S., 2021. Lipid Nanoparticles as Delivery Systems for RNA-Based Vaccines. *Pharmaceutics* 13, 206. <https://doi.org/10.3390/pharmaceutics13020206>.
- Ball, R.L., Bajaj, P., Whitehead, K.A., 2017. Achieving long-term stability of lipid nanoparticles: examining the effect of pH, temperature, and lyophilization. *Int. J. Nanomed.* 12, 305–315. <https://doi.org/10.2147/IJN.S123062>.
- Campillo-Davo, D., de Laere, M., Roex, G., Versteven, M., Flumens, D., Berneman, Z.N., van Tendeloo, V.F.I., Anguille, S., Lion, E., 2021. The Ins and Outs of Messenger RNA Electroporation for Physical Gene Delivery in Immune Cell-Based Therapy. *Pharmaceutics* 13. <https://doi.org/10.3390/pharmaceutics13030396>.
- Cheng, X., Lee, R.J., 2016. The role of helper lipids in lipid nanoparticles (LNPs) designed for oligonucleotide delivery. *Adv. Drug Deliv. Rev.* 99, 129–137. <https://doi.org/10.1016/j.addr.2016.01.022>.

- Das, R., Ge, X., Fei, F., Parvanyan, S., Weissleder, R., Garriss, C.S., 2024. Lipid Nanoparticle-mRNA Engineered Dendritic Cell Based Adoptive Cell Therapy Enhances Cancer Immune Response. *Small methods*, e2400633. <https://doi.org/10.1002/smt.202400633>.
- Das, R., Halabi, E.A., Fredrich, I.R., Oh, J., Peterson, H.M., Ge, X., Scott, E., Kohler, R.H., Garriss, C.S., Weissleder, R., 2023. Hybrid LNP Prime Dendritic Cells for Nucleotide Delivery. *Advanced science (Weinheim, Baden-Wurttemberg, Germany)* 10, e2303576. <https://doi.org/10.1002/adv.202303576>.
- Eygeris, Y., Gupta, M., Kim, J., Sahay, G., 2022. Chemistry of Lipid Nanoparticles for RNA Delivery. *Acc. Chem. Res.* 55, 2–12. <https://doi.org/10.1021/acs.accounts.1c00544>.
- Gote, V., Bolla, P.K., Kommineni, N., Butreddy, A., Nukala, P.K., Palakurthi, S.S., Khan, W., 2023. A Comprehensive Review of mRNA Vaccines. *Int. J. Mol. Sci.* 24. <https://doi.org/10.3390/ijms24032700>.
- Hald Albertsen, C., Kulkarni, J.A., Witzigmann, D., Lind, M., Petersson, K., Simonsen, J. B., 2022. The role of lipid components in lipid nanoparticles for vaccines and gene therapy. *Adv. Drug Deliv. Rev.* 188, 114416. <https://doi.org/10.1016/j.addr.2022.114416>.
- Hobo, W., Novobrantseva, T.I., Fredrix, H., Wong, J., Milstein, S., Epstein-Barash, H., Liu, J., Schaap, N., van der Voort, R., Dolstra, H., 2013. Improving dendritic cell vaccine immunogenicity by silencing PD-1 ligands using siRNA-lipid nanoparticles combined with antigen mRNA electroporation. *Cancer Immunol., Immunother.* : CII 62, 285–297. <https://doi.org/10.1007/s00262-012-1334-1>.
- Hou, X., Zaks, T., Langer, R., Dong, Y., 2021. Lipid nanoparticles for mRNA delivery. *Nat. Rev. Mater.* 6, 1078–1094. <https://doi.org/10.1038/s41578-021-00358-0>.
- Huang, Y., Mahley, R.W., 2014. Apolipoprotein E: structure and function in lipid metabolism, neurobiology, and Alzheimer's diseases. *Neurobiol. Dis.* 72 (Pt A), 3–12. <https://doi.org/10.1016/j.nbd.2014.08.025>.
- Johnson, L.A., Olsen, R.H.J., Merckens, L.S., DeBarber, A., Steiner, R.D., Sullivan, P.M., Maeda, N., Raber, J., 2014. Apolipoprotein E-low density lipoprotein receptor interaction affects spatial memory retention and brain ApoE levels in an isoform-dependent manner. *Neurobiol. Dis.* 64, 150–162. <https://doi.org/10.1016/j.nbd.2013.12.016>.
- Kim, B., Hosn, R.R., Remba, T., Yun, D., Li, N., Abraham, W., Melo, M.B., Cortes, M., Li, B., Zhang, Y., Dong, Y., Irvine, D.J., 2023. Optimization of storage conditions for lipid nanoparticle-formulated self-replicating RNA vaccines. *J. Control. Release* 353, 241–253. <https://doi.org/10.1016/j.jconrel.2022.11.022>.
- Kim, E.H., Teerdhala, S.V., Padilla, M.S., Joseph, R.A., Li, J.J., Haley, R.M., Mitchell, M. J., 2024. Lipid nanoparticle-mediated RNA delivery for immune cell modulation. *Eur. J. Immunol.* 54, e2451008. <https://doi.org/10.1002/eji.202451008>.
- Kim, M., Jeong, M., Hur, S., Cho, Y., Park, J., Jung, H., Seo, Y., Woo, H.A., Nam, K.T., Lee, K., Lee, H., 2021. Engineered ionizable lipid nanoparticles for targeted delivery of RNA therapeutics into different types of cells in the liver. *Sci. Adv.* 7. <https://doi.org/10.1126/sciadv.abf4398>.
- Kitte, R., Rabel, M., Geczy, R., Park, S., Fricke, S., Koehl, U., Tretbar, U.S., 2023. Lipid nanoparticles outperform electroporation in mRNA-based CAR T cell engineering. *Mol. Ther. Methods Clin. Dev.* 31, 101139. <https://doi.org/10.1016/j.omtm.2023.101139>.
- Kon, E., Elia, U., Peer, D., 2022. Principles for designing an optimal mRNA lipid nanoparticle vaccine. *Curr. Opin. Biotechnol.* 73, 329–336. <https://doi.org/10.1016/j.copbio.2021.09.016>.
- Lamparelli, E.P., Ciaglia, E., Ciardulli, M.C., Lopardo, V., Montella, F., Puca, A.A., Della Porta, G., 2025. Optimizing mRNA delivery: A microfluidic exploration of DOTMA vs. DOTAP lipid nanoparticles for GFP expression on human PBMCs and THP-1 cell line. *Int. J. Pharm.* 672, 125324. <https://doi.org/10.1016/j.ijpharm.2025.125324>.
- Lion, E., Anguille, S., Berneman, Z.N., Smits, E.L.J.M., van Tendeloo, V.F.I., 2011. Poly(I:C) enhances the susceptibility of leukemic cells to NK cell cytotoxicity and phagocytosis by DC. *PLoS One* 6, e20952. <https://doi.org/10.1371/journal.pone.0020952>.
- Maeki, M., Uno, S., Niwa, A., Okada, Y., Tokeshi, M., 2022. Microfluidic technologies and devices for lipid nanoparticle-based RNA delivery. *J. Control. Release* 344, 80–96. <https://doi.org/10.1016/j.jconrel.2022.02.017>.
- Mahley, R.W., 1988. Apolipoprotein E: cholesterol transport protein with expanding role in cell biology. *Science (New York, N.Y.)* 240, 622–630. <https://doi.org/10.1126/science.3283935>.
- Mehta, M., Bui, T.A., Yang, X., Aksoy, Y., Goldys, E.M., Deng, W., 2023. Lipid-Based Nanoparticles for Drug/Gene Delivery: An Overview of the Production Techniques and Difficulties Encountered in Their Industrial Development. *ACS Mater. Au* 3, 600–619. <https://doi.org/10.1021/acsmaterialsau.3c00032>.
- Oude Blenke, E., Ørnsvov, E., Schöneich, C., Nilsson, G.A., Volkin, D.B., Mastrobattista, E., Almarsson, Ö., Crommelin, D.J.A., 2023. The Storage and In-Use Stability of mRNA Vaccines and Therapeutics: Not A Cold Case. *J. Pharm. Sci.* 112, 386–403. <https://doi.org/10.1016/j.xphs.2022.11.001>.
- Pardi, N., Hogan, M.J., Porter, F.W., Weissman, D., 2018. mRNA vaccines - a new era in vaccinology. *Nat. Rev. Drug Discov.* 17, 261–279. <https://doi.org/10.1038/nrd.2017.243>.
- Pareja Tello, R., Lamparelli, E.P., Ciardulli, M.C., Hirvonen, J., Barreto, G., Mafulli, N., Della Porta, G., Santos, H.A., 2025. Hybrid lipid nanoparticles derived from human mesenchymal stem cell extracellular vesicles by microfluidic sonication for collagen I mRNA delivery to human tendon progenitor stem cells. *Biomater. Sci.* <https://doi.org/10.1039/d4bm01405g>.
- Sasaki, K., Sato, Y., Okuda, K., Iwakawa, K., Harashima, H., 2022. mRNA-Loaded Lipid Nanoparticles Targeting Dendritic Cells for Cancer Immunotherapy. *Pharmaceutics* 14. <https://doi.org/10.3390/pharmaceutics14081572>.
- Schober, G.B., Story, S., Arya, D.P., 2024. A careful look at lipid nanoparticle characterization: analysis of benchmark formulations for encapsulation of RNA cargo size gradient. *Sci. Rep.* 14, 2403. <https://doi.org/10.1038/s41598-024-52685-1>.
- Sharma, P., Hoorn, D., Aitha, A., Breier, D., Peer, D., 2024. The immunostimulatory nature of mRNA lipid nanoparticles. *Adv. Drug Deliv. Rev.* 205, 115175. <https://doi.org/10.1016/j.addr.2023.115175>.
- Shi, G.-N., Zhang, C.-N., Xu, R., Niu, J.-F., Song, H.-J., Zhang, X.-Y., Wang, W.-W., Wang, Y.-M., Li, C., Wei, X.-Q., Kong, D.-L., 2017. Enhanced antitumor immunity by targeting dendritic cells with tumor cell lysate-loaded chitosan nanoparticles vaccine. *Biomaterials* 113, 191–202. <https://doi.org/10.1016/j.biomaterials.2016.10.047>.
- Smits, E.L., Stein, B., Nijs, G., Lion, E., Van Tendeloo, V.F., Willems, Y., Anguille, S., Berneman, Z.N., 2016. Generation and cryopreservation of clinical grade Wilms' Tumor 1 mRNA-loaded dendritic cell vaccines for cancer immunotherapy. *Tumor Immunology: Methods and Protocols* 27–35. https://doi.org/10.1007/978-1-4939-3338-9_3.
- Sokolowska, E., Blachnio-Zabielska, A.U., 2019. A Critical Review of Electroporation as A Plasmid Delivery System in Mouse Skeletal Muscle. *Int. J. Mol. Sci.* 20. <https://doi.org/10.3390/ijms20112776>.
- Verbeke, R., Lentacker, I., de Smedt, S.C., Dewitte, H., 2019. Three decades of messenger RNA vaccine development. *Nano Today* 28, 100766. <https://doi.org/10.1016/j.nantod.2019.100766>.
- Wang, M.M., Wappelhorst, C.N., Jensen, E.L., Chi, Y.-C.-T., Rouse, J.C., Zou, Q., 2023. Elucidation of lipid nanoparticle surface structure in mRNA vaccines. *Sci. Rep.* 13, 16744. <https://doi.org/10.1038/s41598-023-43898-x>.
- Webb, C., Ip, S., Bathula, N.V., Popova, P., Soriano, S.K.V., Ly, H.H., Eryilmaz, B., Nguyen Huu, V.A., Broadhead, R., Rabel, M., Villamagna, I., Abraham, S., Raeesi, V., Thomas, A., Clarke, S., Ramsay, E.C., Perrie, Y., Blakney, A.K., 2022. Current Status and Future Perspectives on mRNA Drug Manufacturing. *Mol. Pharm.* 19, 1047–1058. <https://doi.org/10.1021/acs.molpharmaceut.2c00010>.
- Zhang, Y., Béliand, L.-C., Roussel, S., Bertrand, N., Hébert, S.S., Vallières, L., 2024. Optimization of a lipid nanoparticle-based protocol for RNA transfection into primary mononuclear phagocytes. *J. Leukoc. Biol.* 115, 1165–1176. <https://doi.org/10.1093/jleuko/qiae059>.